Annals of Biomedical Engineering, Vol. 40, No. 7, July 2012 (© 2012) pp. 1554–1567
DOI: 10.1007/s10439-012-0517-4

Deterioration of Stress Distribution Due to Tunnel Creation in Single-Bundle and Double-Bundle Anterior Cruciate Ligament Reconstructions

JIE YAO,[1,2,3] CHUNYI WEN,[5,6] JASON TAK-MAN CHEUNG,[4] MING ZHANG,[3] YONG HU,[5] CHUNHOI YAN,[5] KWONG-YUEN PETER CHIU,[5] WILLIAM WEIJIA LU,[5,6] and YUBO FAN[1,2]

[1]Key Laboratory for Biomechanics and Mechanobiology of Ministry of Education, School of Biological Science and Medical Engineering, Beihang University, 37 Xueyuan Road, Haidian District, Beijing 100191, China; [2]National Key Laboratory of Virtual Reality Technology, Beihang University, Beijing 100191, China; [3]Department of Health Technology and Informatics, The Hong Kong Polytechnic University, Hung Hom, Kowloon, Hong Kong; [4]Li Ning Sports Science Research Center, Beijing, China; [5]Department of Orthopaedics and Traumatology, Li Ka Shing Faculty of Medicine, The University of Hong Kong, 21 Sassoon Road, Pokfulam, Hong Kong; and [6]Research Center for Human Tissues and Organs Degeneration, Shenzhen Institute of Advanced Technology, Chinese Academy of Science, Shenzhen, China

(*Received 23 September 2011; accepted 16 January 2012; published online 1 February 2012*)

Associate Editor Michael R. Torry oversaw the review of this article.

Abstract—Bone tunnel enlargement is a common effect associated with knee laxity after anterior cruciate ligament (ACL) reconstruction. Nevertheless, its exact pathomechanism remains controversial. One of the possible reasons could be bone remodeling due to tunnel creation, which changes the stress environment in the joint. The present study aims to characterize the deteriorated stress distribution on the articular surface, which is due to tunnel creation after single-bundle or double-bundle ACL reconstruction. The stress distributions in the knee following ACL reconstruction under the compression, rotation, and valgus torques were calculated using a validated three-dimensional finite element (FE) model. The results indicate that, (a) under compression, von Mises stress is decreased at lateral and posteromedial regions of single/anteromedial (AM) tunnel, whereas it is increased at anterior region of single/AM tunnel in tibial subchondral bone; (b) the concentration of tensile stress is transferred from the articular surface to the location of graft fixation, and tensile stress in subchondral plate is decreased after ACL reconstruction; (c) severe stress concentration occurs between AM and posterolateral tunnels following the double-bundle reconstruction, which may contribute to the tunnel communication after surgery. In summary, the present study affirms that the deterioration of stress distribution occurs near the articular surface, which may cause the collapse of the tunnel wall, and lead to tunnel enlargement. The present study provides an insight into the effect of tunnel creation on articular stress deterioration after single-bundle or double-bundle ACL reconstruction. These findings provide knowledge on the effect of tunnel enlargement after ACL reconstruction in the long term.

INTRODUCTION

Anterior cruciate ligament (ACL) injuries are commonly seen in orthopaedic surgery and sports medicine. The rupture of ACL can change the knee kinematics and lead to joint instability.[18,22,35] An ACL deficient knee often results in meniscal injuries and initiation of osteoarthritis (OA).[25] Thus, ACL reconstruction is recommended to restore knee stability, and to lower the risk of OA.[25] Traditionally, ACL reconstruction is performed with a single bundle of graft, which passes through femoral and tibial footprints of the ACL.[13] However, in recent years, natural ACL has been known to be composed of two bundles, namely, anteromedial (AM) and posterolateral (PL) bundles, which maintain the anterior-posterior and rotational stability of the knee, respectively.[9,43] Therefore, there has been an increasing interest in double-bundle ACL reconstruction, which applies two bundles of grafts to restore the function of the AM and PL bundles.[31,39]

However, there have been frequent reports of tunnel enlargement associated with knee laxity after ACL

Address correspondence to William Weijia Lu, Department of Orthopaedics and Traumatology, Li Ka Shing Faculty of Medicine, The University of Hong Kong, 21 Sassoon Road, Pokfulam, Hong Kong and Yubo Fan, Key Laboratory for Biomechanics and Mechanobiology of Ministry of Education, School of Biological Science and Medical Engineering, Beihang University, 37 Xueyuan Road, Haidian District, Beijing 100191, China. Electronic mail: wwlu@hkusua.hku.hk, yubo fan@buaa.edu.cn

J. Yao and C. Wen equally contributed to this work.

reconstruction, which often leads to the reconstruction failure and complicates the revision surgery.[40,42] Its exact pathomechanism remains unclear. Tunnel enlargement could be initiated by micro damages in the bone near the intra-articular tunnel aperture. One of the possible reasons could be the bone remodeling due to tunnel creation, which changes the stress distribution near the articular surface.

The deterioration of the stress distribution after ACL reconstruction was less focused, which is caused by tunnel creation that drills through femur and tibia. These tunneled cavities may interrupt the natural force transmission in the bone. Au *et al.*[3] reported stress alteration occurred around the tibial tunnel wall after the single tunnel creation under the compressive loadings. Abnormal stress distribution near the tunnel may lead to subchondral bone remodeling, which then changes the tunnel morphology according to Wolff's law.[41] Although ACL reconstruction could improve the knee stability and lower the risk of OA,[25] the abnormal stress environment caused by tunnel creation could lead to the tunnel enlargement, and contribute to the fact that risk of OA cannot be completely eliminated.[24] Moreover, double-bundle reconstruction creates double tunnels in the bone, which may aggravate the abnormal stress distribution, although it may restore the knee stability better than that of single-bundle reconstruction. Previous studies have discussed the influence of tunnel placement and morphology on the outcome of ACL reconstruction, and questioned if double-bundle reconstruction is always better than single-bundle reconstruction.[19,31,39,42] However, the stress deterioration after single-bundle or double-bundle ACL reconstruction under different loading conditions has not been thoroughly studied and quantified.

The objective of the present study is to characterize quantitatively the deterioration of stress distribution around the tunnels after either single-bundle or double-bundle ACL reconstruction; different loading conditions are analyzed with a validated FE model of the human knee joint. Graft bundles are included in the FE model, and the longitudinal graft motion between the graft and tunnel wall (bungee effect) was also considered. Focus is placed on the stress alteration near the articular surface, where may be the initial location of tunnel enlargement.

MATERIALS AND METHODS

Image Acquisition

A subject (age: 30 years; mass: 65 kg; height: 172 cm), free from any knee joint disease, volunteered to participate in the present study. Magnetic resonance (MR) image allows researchers to identify soft tissues and the bone shapes, thus the right knee of the subject was scanned by an MR machine (Siemens, Germany) from approximately 20 cm superior to the knee joint line to 20 cm inferior. A total of 65 sagittal T2-weighted images of the knee joint were acquired with the spin echo sequence. The imaging parameters were as follows: field of view (FOV) = 180.5 × 149.5 mm, slice thickness = 2 mm, number of averages = 1, magnetic field = 1.5 T, resolution = 0.47 × 0.47 × 2 mm^3, time of echo (TE)/time of repetition (TR) = 43/7170 ms. The knee was scanned at extension and 45° flexion. A sample of the acquired images is shown in Fig. 1. Images of the knee at extension were used to establish the three-dimensional (3D) FE models, whereas the other images were used for validation. To maintain the knee static and relax during MR scanning, low temperature thermoplastic sheets (ORFIT® Eco, ORFIT, Inc., Belgium), were activated to wrap the femur, knee and tibia. Scanning was performed after the thermoplastic sheets were cooled to room temperature and stiff enough to maintain the knee position. Volunteer gave written, informed consent to this study that approved by the Ethical Committee of The Hong Kong Polytechnic University (Project ID: HSEARS20070115001-01).

Model Establishment

The geometries of the cartilage, meniscus, femur, and tibia, as well as the insertion sites of the ligaments and meniscal horns, were obtained from the MR images, and were analyzed by the image processing software MIMICS (Materialise, Inc., Belgium). The

FIGURE 1. MR image of the human knee joint. Imaging parameters were as follows: FOV = 180.5 × 149.5 mm, slice thickness = 2 mm, number of averages = 1, magnetic field = 1.5 T, resolution = 0.47 × 0.47 × 2 mm^3, TE/TR = 43/7170 ms.

segmentations of the cartilage, meniscus, cancellous bone, and cortical bone were performed according to the grayscales of different tissues under the guidance of a radiologist. The grayscale of cartilage, meniscus, cancellous bone, and cortical bone ranged from approximately 24 to 68, 0 to 39, 39 to 160, and 0 to 25, respectively. The geometry of the knee at extension was applied to reconstruct the 3D FE model using the FE software ABAQUS (Simulia, Inc., USA). The femur, tibia, meniscus and cartilage were meshed into four-node tetrahedral elements. The ACL (both AM and PL bundles), posterior cruciate ligament (PCL), medial collateral ligament (MCL), lateral collateral ligament (LCL), and meniscal horns were modeled as bundles of one-dimensional nonlinear elements.[28,44] The material properties for the model were cited from literature. The cartilage was assumed to behave as a linear isotropic elastic material with a Young's Modulus of 5 MPa and a Poisson ratio of 0.35.[44] The meniscus was modeled as a transversely isotropic, linear elastic, homogeneous material, with a circumferential modulus (E_θ) of 125 MPa, and both the radio modulus (E_R) and axial modulus (E_Z) of 27.5 MPa; Poisson ratios $v_{\theta R}$, $v_{\theta Z}$ and v_{RZ} were 0.1, 0.1 and 0.33, respectively; both the shear modulus $G_{\theta R}$ and $G_{\theta Z}$ were 2 MPa.[44] The lateral anterior (LA), lateral posterior (LP), medial anterior (MA) and medial posterior (MP) horn attachments of the meniscus were modeled as one-dimensional nonlinear elastic elements with the tensile modulus of 600 MPa. The initial lengths of the four attachments were respectively assumed to be 8.2, 14.7, 14.0, and 9.8 mm, whereas the cross-sectional areas were 8.6, 11.8, 14.8, and 8.63 mm^2.[28] The ligaments were also simulated as one-dimensional nonlinear elements. Ligament strain was defined as $\varepsilon = \Delta L/L_0$, whereas ΔL is the deformation of the length, and L_0 is the initial length of the ligament (zero load length).[4] Since the ligaments are subject to residual strain *in vivo*, which is approximately 3–5% in the diarthrodial joints, 3% initial strain (ε_i) was applied based on the literature.[37] Zero load length L_0 was calculated with ε_i and reference length L_i (length of one-dimensional ligament element before applying external loading). $\varepsilon_i = (L_i - L_0)/L_0$, hence, $L_0 = L_i/(1 + \varepsilon_i)$.

The force-strain relationship is described as Eq. (1),

$$f = \begin{cases} \frac{1}{4}k\varepsilon^2/\varepsilon_1, & 0 \le \varepsilon \ll 2\varepsilon_1, \\ k(\varepsilon - \varepsilon_1), & \varepsilon > 2\varepsilon_1, \\ 0, & \varepsilon < 0, \end{cases} \quad (1)$$

where k is a stiff parameter and ε_l is the nonlinear strain level parameter assumed to be 0.03. Equation (1) and the stiff parameters of ACL (both AM and PL bundles), PCL, MCL, and LCL were cited from the literatures.[4,22,28] In addition, the subchondral plate could be a predisposing factor of the articular cartilage degeneration,[5,8,32,33] but it was difficult to identify in the MR images, therefore, the thickness of the subchondral bone was assumed to be 1.5 mm.[27] The subchondral bone was assumed to behave as a linear isotropic elastic material with a Young's Modulus of 1.15 GPa and a Poisson ratio of 0.25.[3] The cancellous bone was modeled as a linear isotropic elastic material with a Young's Modulus of 0.4 GPa and a Poisson ratio of 0.33. The cortical bone was modeled as a linear isotropic elastic material with a Young's Modulus of 17 GPa and a Poisson ratio of 0.33.[38] The contact condition was set between the femur and tibia, the femur and meniscus, and the tibia and meniscus. The tangential behavior was defined as frictionless. The contact pressures-overclosure relationship was defined as "hard" contact, which implies that contact surfaces transmit no contact pressure unless the slave surface comes in contact with the master surface. The sliding formulation was defined as "finite sliding," because of the considerable sliding between the contact pairs.[10] The contact constraint enforcement method was defined as "penalty" method, which could mitigate overconstraint and reduce the number of iterations during analysis.[1] The element size was approximately 2 mm in the distal femur and proximal tibia near the articular surface, and approximately 5 mm in the proximal femur and distal tibia. Alternatively, the element size was approximately 1 mm in the cartilage and tunnel wall. The entire model consisted of 22,418 nodes and 102,219 elements (Fig. 2).

Model Validation

Two methods were designed to validate the developed FE model. Method A: A knee flexion was simulated with the FE model. The meniscal deformations predicted by the FE model were compared with that obtained from the MR images. Method B: The tibial contact areas under compressive loadings were compared with the experimental data obtained from the literature.[14]

Method A: To simulate the knee flexion from 0° to 45°, femoral and tibial displacements were applied as the loading and boundary conditions. In detail, the distal tibia was fixed at six degrees of freedom (DOFs); the femur was flexed from 0° to 45°. The femoral displacement (femur moving from extension to 45° flexion) was determined by two 3D MR models taken at 0° (Fig. 3a) and 45° (Fig. 3b) flexion; these two 3D models were placed in a common coordinate system for comparison (Fig. 3c); femoral displacement was then calculated with the reverse engineering software RAPIDFORM (INUS Technology, Inc., Korea).

To verify the FE model, 3D-shape of the meniscus after the knee was flexed to 45° generated by the FE

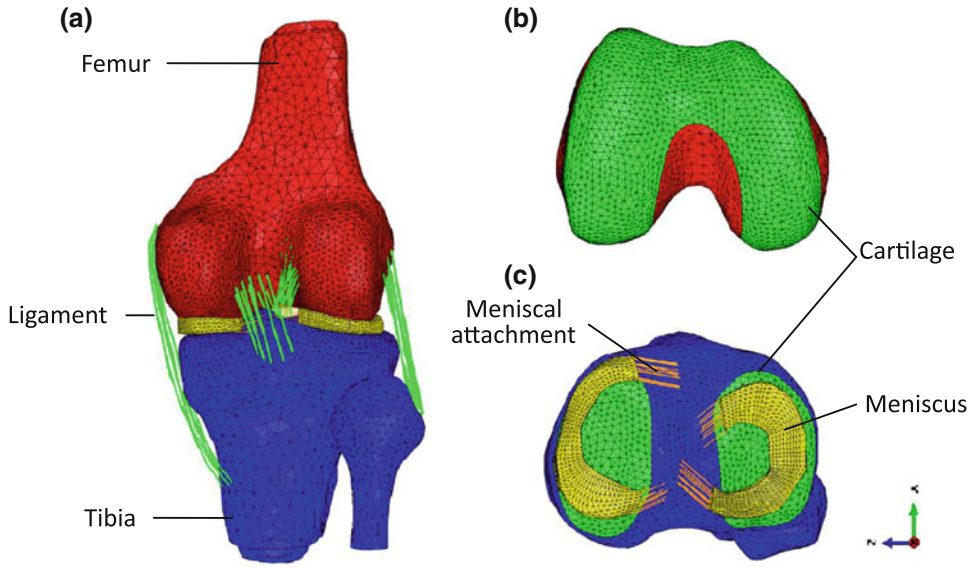

FIGURE 2. 3D FE model of the human knee joint. (a) Intact knee joint. (b) Distal femur. (c) Proximal tibia.

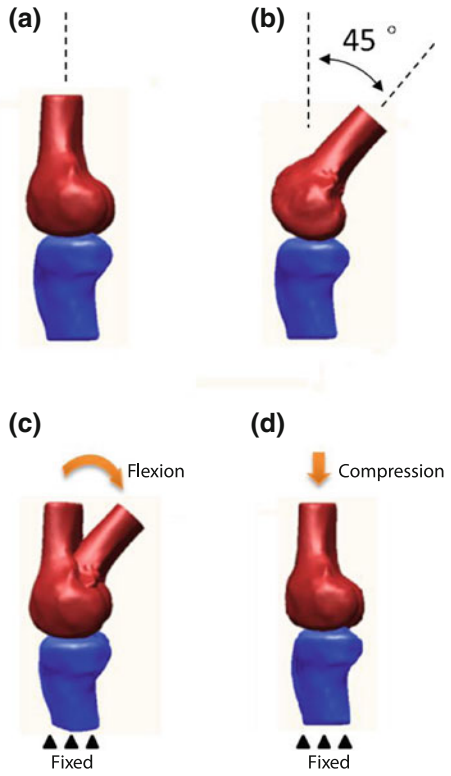

FIGURE 3. Validations of the FE model. (a) 3D model of knee joint at extension. (b) 3D model of knee joint at 45° flexion. (c) Loading and boundary conditions in Method A. Distal tibia was fixed at 6 DOFs, femoral displacement (at 6 DOFs) relative to the tibia was applied on the proximal femur. (d) Loading and boundary conditions in Method B. Distal tibia was fixed at 6 DOFs and proximal femur was fixed at 5 DOFs, with free movement only in proximal–distal direction. Compressive loadings of 200, 500, and 1000 N were applied on proximal femur, along the axis of femoral shaft.

model was compared with the MR images. The degree of agreement was taken as the amount of overlapped volume.

Method B: To compare the tibial contact area in FE model and the experimental results from literature,[14] boundary conditions were applied according to the experimental configuration. The distal tibia was fixed at 6 DOFs, and the proximal femur was fixed at 5 DOFs, with only free to move in proximal–distal direction (Fig. 3d). Compressive loadings of 200, 500, and 1000 N were applied along the axis of the femoral shaft on the proximal femur. The contact areas were the sum of the tibia-meniscus and tibia-femur contact areas.

Simulation of Single-Bundle and Double-Bundle ACL Reconstruction

Single-bundle and double-bundle ACL reconstructions were performed virtually on the validated model according to the surgical procedures in literature.[11,20,39] In single-bundle case, tunnels with a diameter of 8 mm were created. The femoral tunnel was drilled from the virtual accessory anteromedial (AAM) portal and through the center of the AM femoral insertion site at 120° of knee flexion. In the extension model, the angle between the tunnel axis and transverse plane was approximately 37°, the angle between the tunnel axis and sagittal plane was approximately 48°. The tibial tunnel was drilled from the medial site of the tibial tubercle through the center of the AM tibial insertion site. In double-bundle case, the AM and PL tunnels were created, with diameters of 8 mm and 6 mm, respectively. The PL femoral

tunnel was drilled from the virtual AAM portal through the PL femoral footprint at 110° of knee flexion. In the extension model, the angle between the PL tunnel axis and transverse plane was approximately 33°, the angle between the PL tunnel axis and sagittal plane was approximately 53°. The AM femoral tunnel was drilled from the virtual AAM portal through the AM femoral footprint at 120° of knee flexion.[31] In the extension model, the angle between the AM tunnel axis and transverse plane was approximately 37°, the angle between the AM tunnel axis and sagittal plane was approximately 48°. The PL tibial tunnel was drilled from the anterior site of the superficial MCL, and through the PL tibial footprint. The AM tibial tunnel was drilled from the medial site of the tibial tubercle, and through the AM tibial footprint (Figs. 4a and 4b).

The present study focuses on the influence of tunnel on the stress aggravation, and would like to eliminate the side effect of the graft and screws; hence, each bundle of graft was modeled as one-dimensional nonlinear elements, with the same material property as the ACL. The grafts were guided through the tunnels and fixed at the bone with a distance of 25 mm from the extra-articular side of the tunnels, which was the length of the screw. As shown in Figs. 4c and 4d, since the screws' effect was to pressurize and fix the extra-articular part of graft (part "L") onto the tunnel wall, only the component between the screw tip and intra-articular tunnel aperture (part "M") of the graft was free to deform like a ligament. Thus, part 'L' of the graft was fixed onto the tunnel wall and the screws themselves were not analyzed. The slipring connector algorithm was implemented in the FE software ABAQUS to simulate the graft longitudinal slipping on the edge of intra-articular tunnel aperture. The "slipring connector" was a constraint method that allowed the belt-like element (such as the graft in the present study) to flow or rotate freely upon a point.[2]

Three typical loadings were applied to compare the responses of the intact knee and the knee with ACL reconstruction. (a) With the distal tibia fixed, a compressive force of 1500 N was applied through the axis

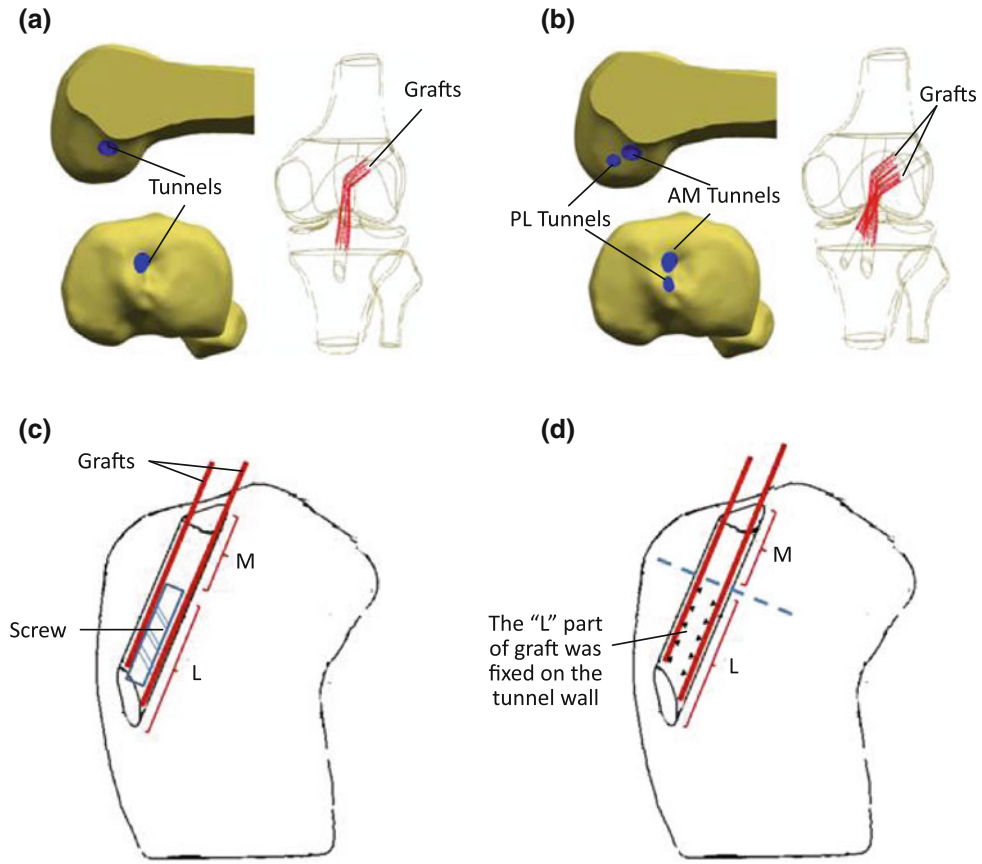

FIGURE 4. Simulations of the ACL reconstruction. (a) Single-bundle ACL reconstruction. (b) Double-bundle ACL reconstruction. The grafts were modeled with one-dimensional elements. (c) Diagram of graft fixation. The graft in the tunnel is divided into two parts, "L" part is from the extra-articular tunnel aperture to the screw tip, which is pressurized and fixed onto the tunnel wall by screw, and "M" part is from the screw tip to the intra-articular tunnel aperture, which is free to deform like a ligament. (d) Simplification of graft fixation. "L" part of graft is fixed on the tunnel wall, and the screw itself was not analyzed. Blue line indicates the location of screw tip.

of the femoral shaft onto the proximal femur; (b) with the proximal femur fixed, an internal rotation moment of 1.1% body weight times meter (BWm) was applied at the distal tibia, which is the peak value of rotation during a normal walking cycle[21]; (c) with the proximal femur fixed, an abducting moment of 1.0% BWm was applied at the distal tibia, which was also the peak value of valgus during a normal walking cycle.[21] The calculations were carried out using the ABAQUS.

RESULTS

Validation

For Method A, the 3D-shape of the meniscus at 45° knee flexion was predicted by the FE model and compared with that from the MR images (Fig. 5). The overlapped volume was 88% for the medial meniscus, and 83.5% for the lateral meniscus. These mismatch volumes are within the range of the MR image pixel resolution (0.469 mm), as explained in literature.[28,44] Briefly, one pixel inferior shift of meniscus could generate a 12.36% volume mismatch for the medial meniscus and a 22.9% volume mismatch for the lateral meniscus. Thus, the developed FE model was verified.

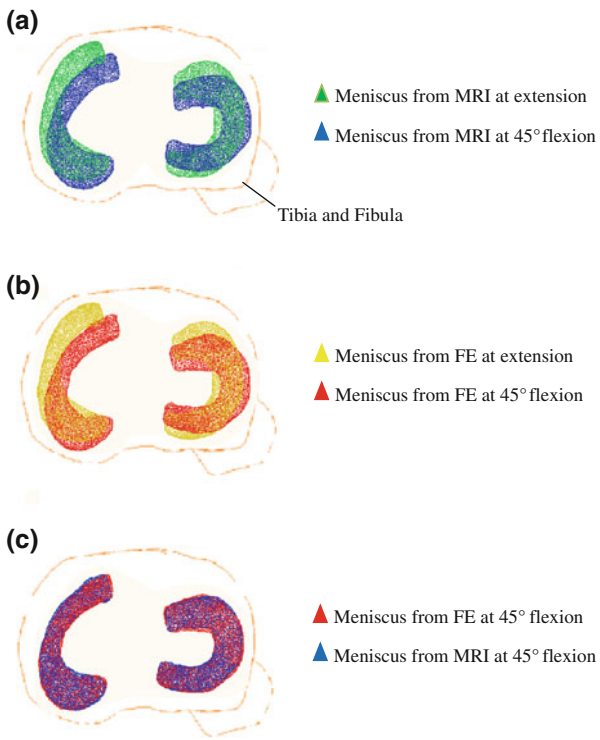

FIGURE 5. Result of the validation (Method A). (a) Meniscus from MRI at 0° (green) and 45° (blue) flexion. (b) Meniscus from FE at 0° (yellow) and 45° (red) flexion. (c) 3D-shape of meniscus at 45° flexion predicted by FE model (red) was compared with that from MRI (blue). The overlapped volume was 88% for medial meniscus, and 83.5% for the lateral meniscus.

For Method B, the contact areas on the tibial plateau obtained from the FE model were compared with that in the experimental study in literature. As shown in Fig. 6, under the compressive loadings of 200, 500, and 1000 N the contact areas in the medial side of tibial plateau were 394.2, 497.7, and 583.8 mm^2, respectively; and the contact areas in the lateral side of tibial plateau were 220.8, 433.9, and 563.1 mm^2, respectively. The FE results were in the range for the experimental average deviations.[14]

ACL Reconstruction

To understand the effect of tunnel creation on the stress disruption after ACL reconstruction, the changes in stress distribution between the single-bundle and double-bundle cases were compared. The degree of stress increment was defined as $\theta = \frac{\sigma_r - \sigma_i}{\sigma_i} \times 100\%$, where σ_i is the nodal von Mises stress in the intact knee, and σ_r is the nodal von Mises stress after ACL reconstruction. The θ distributions of single-bundle and double-bundle cases under the compressive force of 1500 N are shown in Figs. 7a and 7b. For single-bundle case, the von Mises stress was increased at the anterior site of the tunnel, with a peak value of +116.6%. For double-bundle case, the stress was similarly increased at the anterior site of AM tunnel with a maximum value of +122.6%. Moreover, a severe stress concentration occurred between the AM and PL tunnels, with a peak value of +231.4%. The high stress regions in both cases were located near the tibial subchondral plate around the tunnels. The θ distributions in the tibial subchondral plate are shown in Figs. 7c and 7d. The stress was decreased at the posteromedial region (by approximately 33.3% in the single-bundle case and approximately 14.1% in the double-bundle case) and the lateral region (by approximately 77.8% in the single-bundle case and approximately 74.4% in the double-bundle case) of the single/AM tunnel. In particular, stress in the double-bundle case was further decreased at the posterolateral region of the PL tunnel with a peak value of −53.7%. Figure 8 shows the θ distributions at the femoral sagittal section. In the single-bundle case, stress was increased by approximately 80.7% in the proximal region of tunnel, while it was decreased by approximately 24.7% in the distal region of tunnel. In the double-bundle case, PL tunnel creation aggravated this stress decreasing to −57.0%, and led to a stress concentration (by approximately 94.4%) at its posterior region.

To understand the effect of different loading conditions on stress disruption, θ distributions under rotational moments were calculated. As shown in Figs. 9a and 9b, after either the single-bundle or

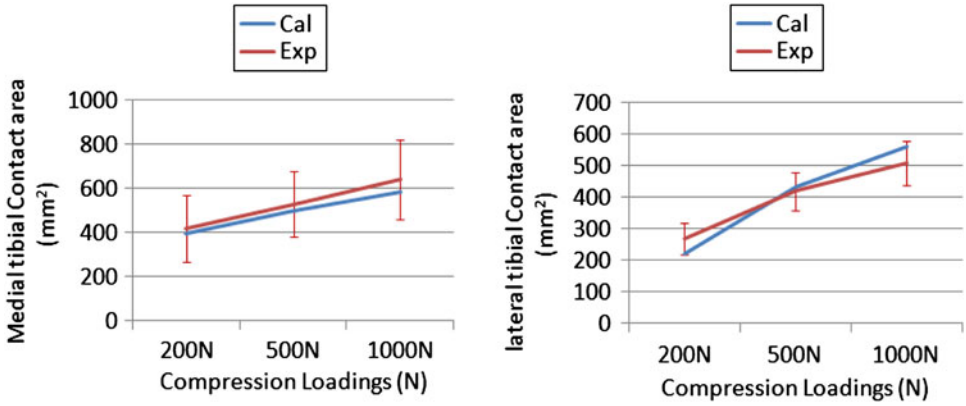

FIGURE 6. Results of the validation (Method B). The contact areas in tibial plateau from FE model (blue) were compared with that from experiment (red) in literature.[14] (a) Contact area in the medial side of tibial plateau. (b) Contact area in the lateral side of tibial plateau. The FE results were in the range of experimental average deviations.

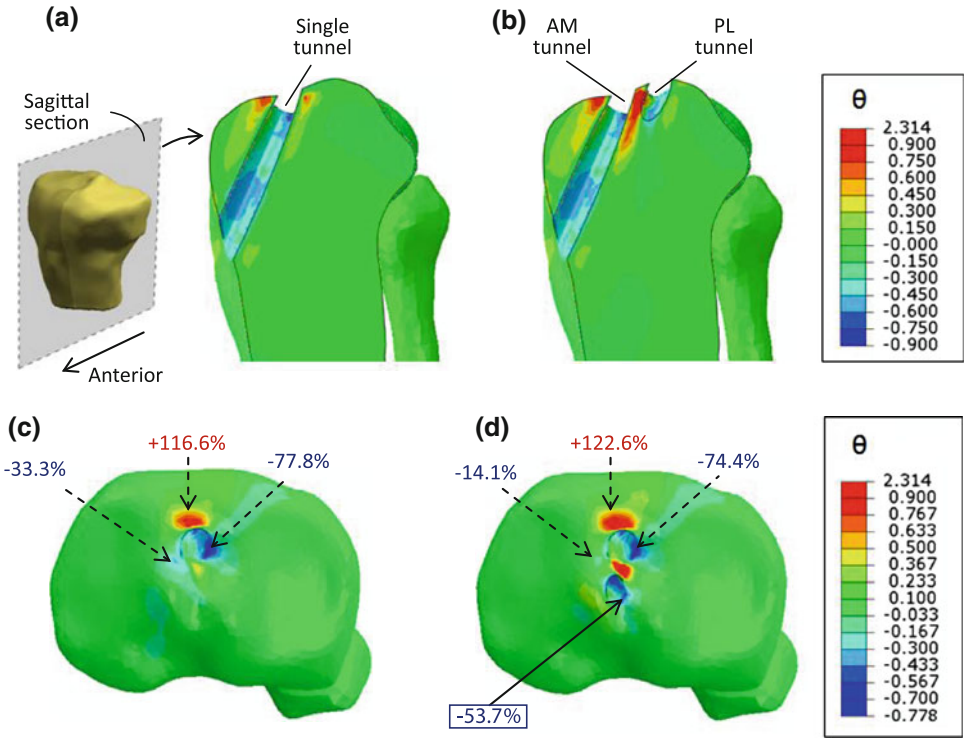

FIGURE 7. Distributions of stress increment degree (θ) in tibial sagittal section (a, b) and tibial plateau (c, d) under compression loading of 1500 N. θ was defined as $\theta = \frac{\sigma_r - \sigma_i}{\sigma_i} \times 100\%$, where σ_i is the nodal von Mises stress of intact knee, and σ_r is the nodal von Mises stress after ACL reconstruction. (a) Single-bundle case. (b) Double-bundle case. Von Mises stress was increased remarkably by about 231.4% between AM and PL tunnels. (c) Single-bundle case. (b) Double-bundle case. Von Mises stress was increased at the anterior region of the single/AM tunnel, but it was decreased at the posteromedial and lateral region of single/AM tunnel. In the double-bundle case, stress was further decreased in the posterolateral region of PL tunnel with its peak value of −53.7%.

double-bundle ACL reconstruction, the degree of stress increment (θ) was consistently high (>200%) in the middle of each tunnel, which was located at the graft fixation (blue dashed line in Fig. 4d). However, θ was consistently low in the proximal tibial around the tunnel, which was close to the footprint of the natural ACL. Furthermore, although stress in the tibial plateau was decreased in both cases (Figs. 9c and 9d), it was less severe in the double-bundle reconstruction. θ in the lateral region of AM tunnel was also decreased from +312.7 to +178.4%. Similarly, stress in the femur was increased near the graft fixation, as well as the posterior region of AM tunnel (by about +184.5%). The stress around the PL tunnel was restored in double-bundle reconstruction compared with that of single-bundle case.

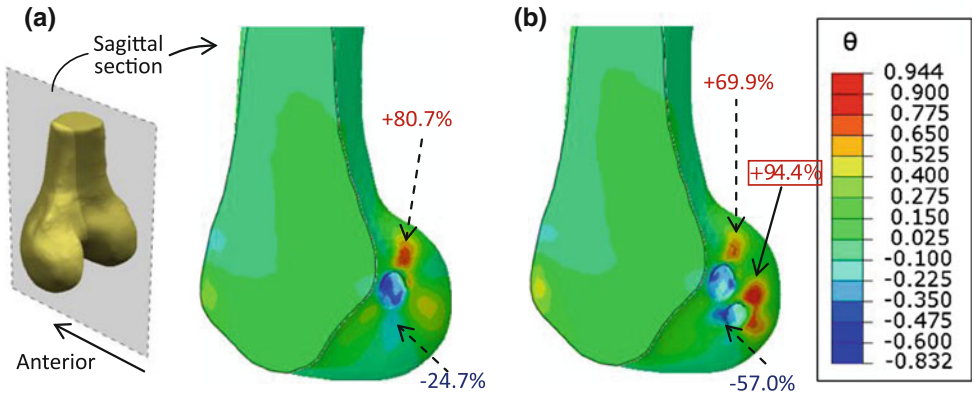

FIGURE 8. Distribution of stress increment degree (θ) in the sagittal section of femur under compression loading of 1500 N. (a) Distribution of θ in single-bundle case. Stress was increased by about 80.7% at proximal region of tunnel, while was decreased by about 24.7% at distal region of tunnel. (b) Distribution of θ in double-bundle case. PL tunnel creation aggravated this stress decreasing to −57.0%, and led to a stress concentration (by about 94.4%) at its posterior region.

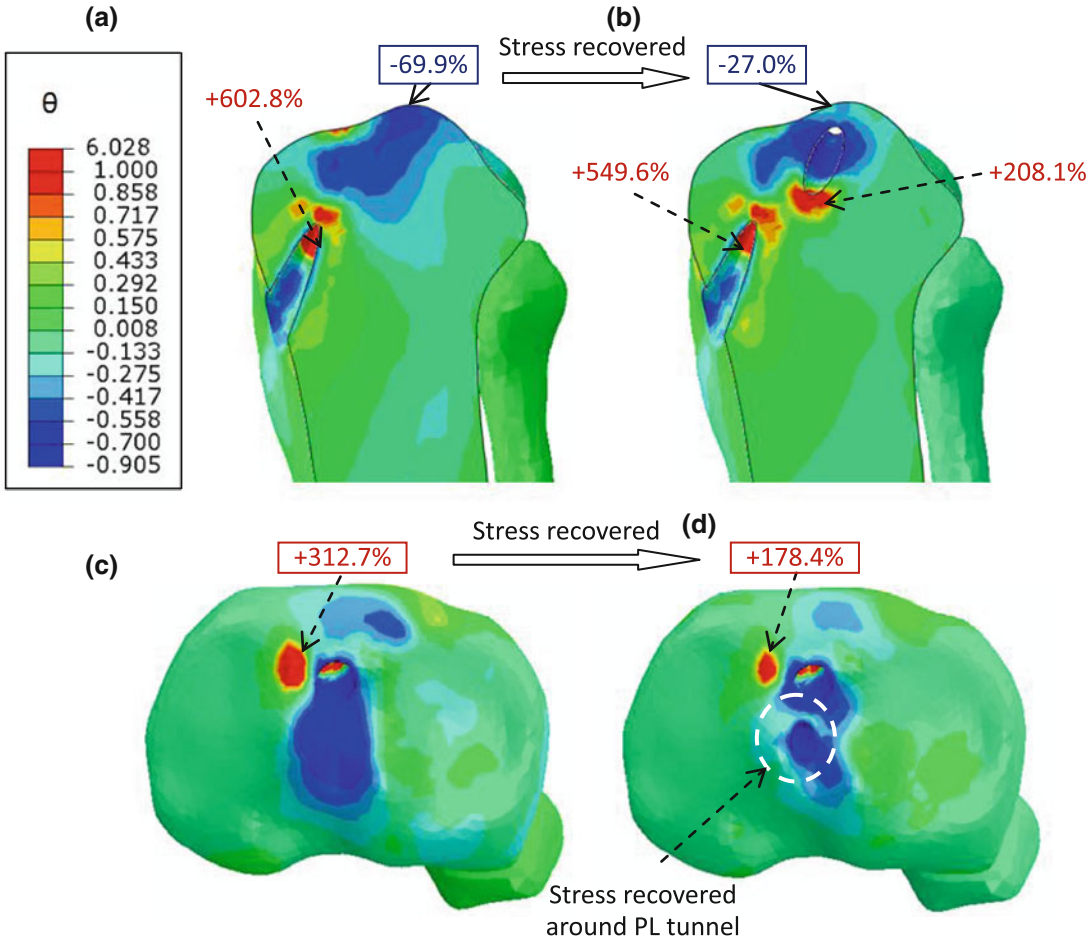

FIGURE 9. Distribution of stress increment degree (θ) in the tibia under rotational torque of 1.1% BWm. (a) Tibial sagittal section in single-bundle case. (b) Tibial sagittal section in double-bundle case. The θ was consistently high in the middle of each tunnel, which was the location of graft fixation, while θ was consistently low in the proximal tibial around the tunnel, which was closed to the footprint of the natural ACL. (c) Tibial plateau in single-bundle case. (d) Tibial plateau in double-bundle case. Double-bundle reconstruction restored the stress around the PL tunnel (white circle), as well as the stress at the lateral region of AM tunnel (from 312.7 to 178.4%).

According to Wolff's law, not only the stress intensity, but also its trajectory is closely related to bone remodeling.[41] The trajectories of first and third principle stresses are shown in Fig. 10. In the intact knee, the first principle stress (blue arrows) was concentrated near the natural footprint of the ACL, and its orientation was similar to the ACL. This local tensile status indicates the ACL force applied on the bone. In the ACL reconstruction cases, however, the first principle stress was concentrated in the middle of each tunnel near the location of graft fixation, which may be caused by the tensile force of the grafts applied on the bones. Moreover, the stress orientation still differed from the normal knee although the stress magnitude was recovered after the PL tunnel creation. In the ACL footprint, the tensile force generated by the natural ligament was replaced by the shear forces between the bone and grafts, where an abnormal remodeling could occur due to the change in stress orientation.

Similar stress environment was observed when applying the valgus torque. As shown in Figs. 11a and 11b, stress near the graft fixation in both cases was increased by more than 200%, whereas the stress in the posterior region of the single/AM tunnel near the tibial subchondral plate was decreased by more than 40%. In particular, the decreasing of stress near the PL tunnel was recovered in double-bundle case. Although the stress magnitude was restored locally, its stress orientation still differed from that of the intact knee (Figs. 11c–11e).

DISCUSSION

In both single-bundle and double-bundle cases, tunnel creations considerably influenced the local biomechanical environment in the knee joint. This influence was more severe near the articular surface, which was the high-risk region for tunnel enlargement. In

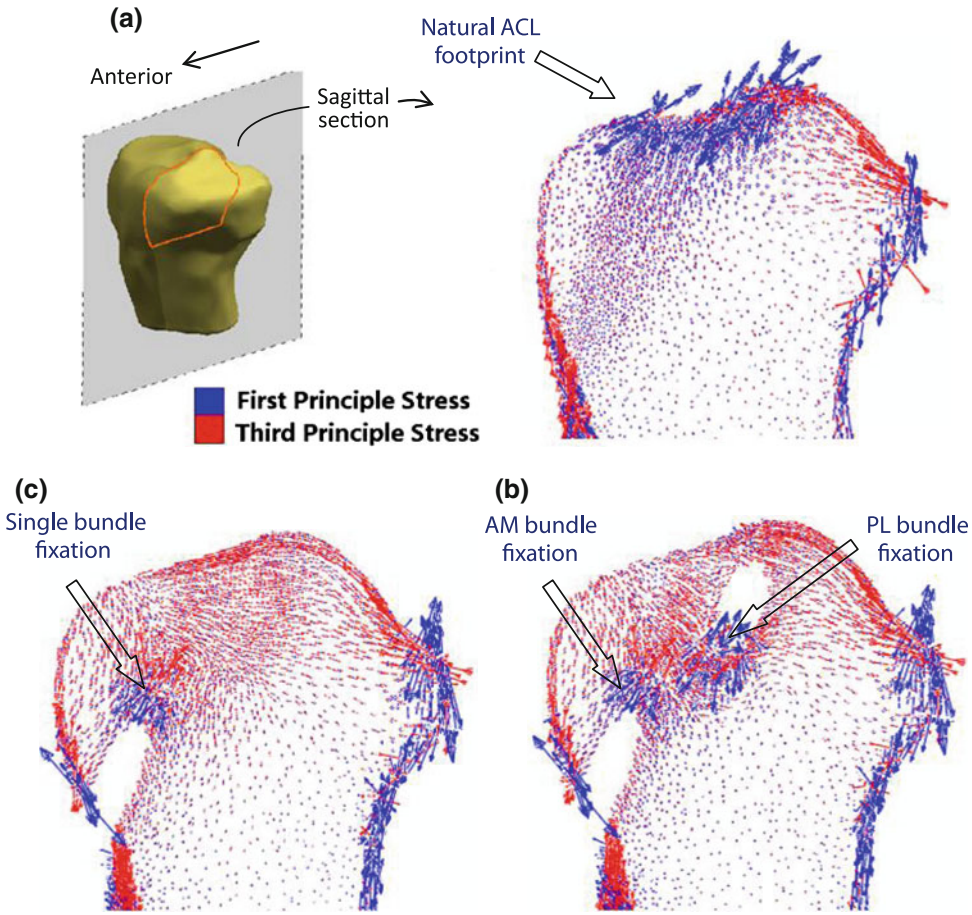

FIGURE 10. Trajectory of first and third principle stress in tibial sagittal sections under an internal rotation torque of 1.1% BWm. Where first principle stress mainly indicates the tensile force (blue arrows), and third principle stress mainly indicates the compressive force (red arrows). (a) Intact knee. (b) Single-bundle case. (c) Double-bundle case. In the intact knee, the first principle stress concentrated near the natural footprint of ACL, with its orientation similar to the ACL. Whereas in the ACL reconstruction cases, the first principle stress concentrated near the location of graft fixation, which could be caused by the force of grafts applied on bones.

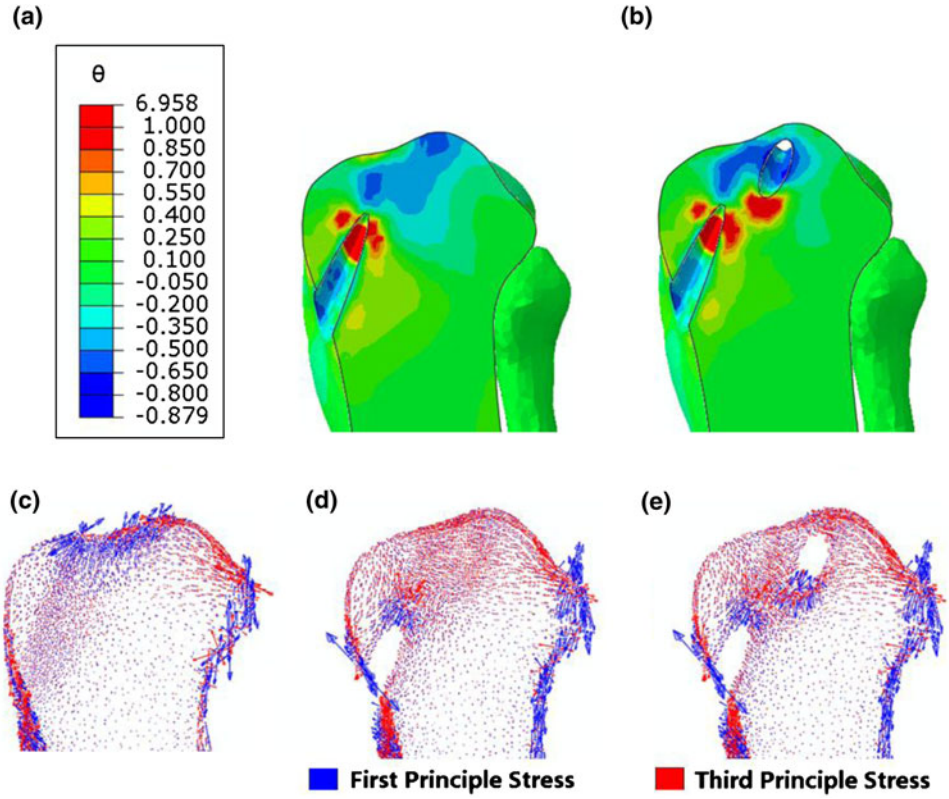

FIGURE 11. FE results under a valgus torque of 1.0% BWm in tibial sagittal section. (a) Distribution of θ in single-bundle case. (b) Distribution of θ in double-bundle case. In both cases, stress was increased near the location of graft fixation, whereas it was decreased in the posterior region of AM tunnel near the tibial subchondral plate. In double-bundle case, the decreasing of stress recovered near the PL tunnel. (c) Trajectory of first and third principle stress of intact tibia. (d) Trajectory of first and third principle stress in single-bundle case. (e) Trajectory of first and third principle stress in double-bundle case. Although double-bundle case restored stress magnitude locally, however, the stress orientations still differ from that of intact knee.

single-bundle reconstruction, stress was increased in the anterior region of tibial tunnel, but was decreased at the lateral and posteromedial region of tibial tunnel under compressive loading (Fig. 7). The knee joint usually experiences compressive loading in daily activities, hence, the permanent alternation of stress distribution could influence the normal bone remodeling. High stress causes bone growth and low stress causes bone loss,[12,41] therefore, (a) subchondral bone in low stress region may collapse and could lead to tunnel enlargement after ACL reconstruction; (b) the subchondral bone thickening would be promoted in high stress region. Some researchers propose that subchondral bone thickening may be one of the predisposing factors of OA, and could be a key target for treatment.[5,8,32,33] Thus, the altered subchondral morphology and property due to increased stress may increase the risk of OA after surgery; (c) bone remodeling around the tunnel may be changed due to nonuniform stress alteration after ACL reconstruction. The nonuniform bone growth and resorption may change the morphology of the intra-articular tunnel apertures in the long term. Kopf *et al.*[19] suggests that an improper tunnel aperture could increase the risk of the damaging surrounding structures. However, the consequence of changing the tunnel morphology could be quite complex combined with the effect of graft-tunnel slipping motion. Therefore, this phenomenon shall be investigated in future *in vivo* experiments.

Stress deterioration near the AM tunnel was similar between the double-bundle and single-bundle cases; however, double-bundle case further aggravated the stress environment around PL tunnels. Severe stress concentration was observed between the AM and PL tunnels in the subchondral bone under compressive loading. According to Frost's mechanostat theory,[12] loading above the critical threshold would, by contrast, lead to micro-damages in the subchondral bone, although high stress may induce bone growth. Clinically, tunnel communication occurs frequently after ACL reconstruction, which may be induced by the severe stress concentration between the AM and PL tunnels. However, the individual difference of bone remodeling and joint mechanics may explain why tunnel communication did not always occur after double-bundle reconstruction.

Furthermore, the concentration of tensile stress was transmitted from the natural ACL footprint to the location of the graft fixation after ACL reconstruction (Figs. 9, 10, and 11). The *in situ* force between the ACL and bone was previously located at the footprint, whereas the *in situ* force between the graft and bone was located at the middle of the tunnels after ACL reconstruction. This alteration decreased the tensile stress around the tunnels in the subchondral plate, which may contribute to the subchondral bone resorption. The comparison of stress trajectories (Fig. 10) indicates that not only the magnitude of stress, but also its orientation was altered at the articular surface after ACL reconstruction. Thus, the abnormal of stress orientation would have an influence on the bone remodeling, and may lead to tunnel enlargement.

The placement of tunnel enlargement observed clinically is varied. Some researchers reported no significant difference of the tunnel enlargement between the sagittal and coronal plane,[36] whereas some others found the tibial tunnel widening in the sagittal plane to be more severe than that in the coronal plane.[17] Based on the calculated results, compressive loading could lead to the tibial stress shielding in the coronal plane (Figs. 7c and 7d), whereas rotational and valgus loadings could lead to the tibial stress shielding in sagittal plane (Figs. 9c, 9d and Figs. 11a and 11b). The sagittal stress shielding under rotation and valgus was more severe than the coronal stress shielding under the compression. The results indicate that the placement and morphology of the tunnel enlargement may be related to individual activities; the contributions of the rotational and valgus loadings to tunnel enlargement in sagittal plane should be more considerable. Siebold *et al.*[36] reported that tunnel communications occurred in 41% of patients after double-bundle ACL reconstruction, which is consistent with the severe stress concentration obtained from the present FE study.

Some researchers believe that there are relationships between strain energy density and bone remodeling,[6,16] and some others propose several bone remodeling theories according to strain and stress.[7,12] To characterize the influence of tunnel creation on the biomechanical environment with various approaches, the increment degree of energy density, equivalent strain and von Mises stress are shown in Fig. 12. The equivalent strain was defined as $\varepsilon = \sqrt{\frac{1}{2}[(\varepsilon_1-\varepsilon_2)^2+(\varepsilon_2-\varepsilon_3)^2+(\varepsilon_3-\varepsilon_1)^2]}$, where ε_1, ε_2 and ε_3 are three principle strains.[26] The trends of the increment degree were similar in all three parameters. The peak of the increment degree was consistently located between AM and PL tunnels, whereas the peak of the decrement degree was consistently located at the lateral side of the AM tunnel and the posterior side of the PL tunnel near the articular surface. Furthermore, the minimum equivalent strain at the posterior region of the PL tunnel was approximately 300 $\mu\varepsilon$ (micro strain), which was comparable to the threshold of bone resorption; Alternatively, the maximum equivalent strain between the AM and PL tunnels was approximately 2900 $\mu\varepsilon$ in the cancellous bone, which was comparable to the threshold of unrepaired micro-fatigue damage.[12] The predicted results may help to understand tunnel enlargement and tunnel communication following surgery.

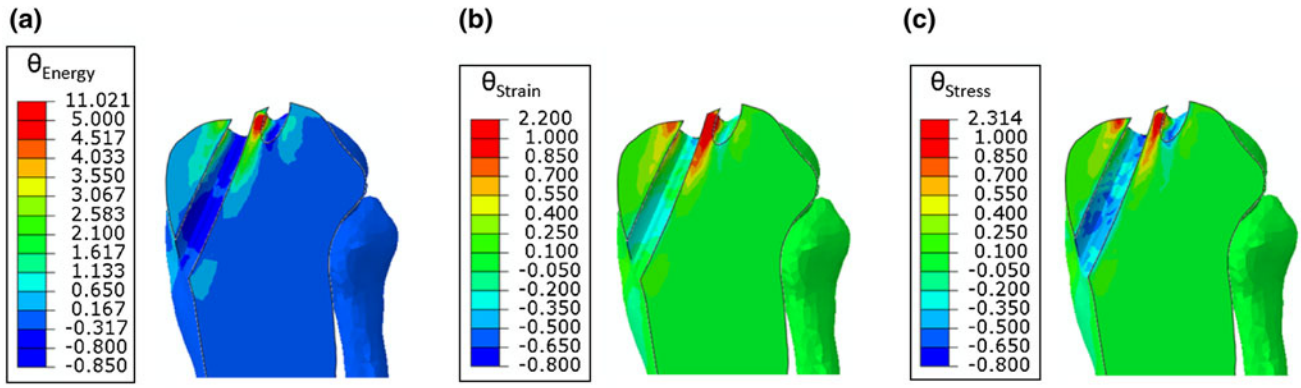

FIGURE 12. Increment degree of strain energy density (a), equivalent strain (b) and von Mises stress (c) in the tibial sagittal section under the compressive loading of 1500 N. (a) Increment degree of strain energy density is defined as $\theta_{Energy} = \frac{E_r - E_i}{E_i} \times 100\%$, where E_i is strain energy density of intact knee, and E_r is strain energy density after ACL reconstruction. (b) Increment degree of equivalent strain is defined as $\theta_{Strain} = \frac{\varepsilon_r - \varepsilon_i}{\varepsilon_i} \times 100\%$, where ε_i is equivalent strain of intact knee, and ε_r is the equivalent strain after ACL reconstruction. Equivalent strain is defined as $\varepsilon = \sqrt{\frac{1}{2}[(\varepsilon_1-\varepsilon_2)^2+(\varepsilon_2-\varepsilon_3)^2+(\varepsilon_3-\varepsilon_1)^2]}$, where ε_1, ε_2 and ε_3 are three principle strains[26]; (c) Increment degree of stress is defined as Fig. 7. The trends of increment degree were similar in all three views, the maximum value of θ consistently located between the AM and PL tunnels, while the minimum value of θ consistently located at the lateral site of AM tunnel and posterior site of PL tunnel near the articular surface.

The FE model in the present study was validated by comparing the meniscal deformation to the MR images, and by comparing the calculated tibial contact area to experimental results. The mismatch volume of the meniscus between the FE results and MR images was also considered. Graft bundles were included in the model, as well as the bungee effect of the graft-tunnel motion. The bungee effect influences the articular stress distribution in the intra-articular tunnel aperture; however, this information is seldom considered in previous FE studies.

The material properties applied to the FE model are cited from literature. However, a range of properties could be found for each tissue, depending on the loading rate and experimental conditions. For the cartilage, the elastic moduli ranging from 5 to 15 MPa have been reported in previous studies.[10,23,28,30,44] The modulus of a viscoelastic material increases with loading rate,[29] thus, the low modulus of the cartilage (5 MPa) was chosen to simulate the quasistatic loading conditions in the present study. For the meniscus, both isotropic and transverse isotropic properties have been applied previously.[28,30,44] The transverse isotropic property was applied in the present study because it could be more accurate when the meniscus is in response to transverse loadings (rotation and valgus). Moreover, the bone material properties applied in the present study are cited from literature that performed similar loading conditions.[3,38] The sensitivity of the stress to the bone material properties was further characterized though the sensitivity analysis. Consequently, changing the Young's Modulus of the cortical bone by ±50% resulted in an alteration of the peak stress within ±10%; changing the Young's Modulus of the subchondral bone by ±50% resulted in an alteration of the peak stress within ±1%; changing the Young's Modulus of the cancellous bone by ±50% resulted in an alteration of the peak stress within ±7%. In addition, the θ distribution trends remained unchanged. The results of the sensitivity analysis show that the trends of the stress deterioration are valid, even with slight variation in bone material properties.

However, there are limitations in the present study. The cortical, subchondral, and cancellous bones were assumed to be isotropic homogeneous materials. Some studies have reported peripheral and longitudinal variations in bone stiffness,[15,34] which may influence the calculated results. However, the trends of stress concentration and shielding near the intra-articular tunnel aperture should be valid. Static algorithm was applied for the simulation; however, practical activities are often dynamic processes. Nevertheless, the static and dynamic results are comparable while the loading rate is low. Furthermore, the loading conditions in the present study are compression, rotation, and valgus torque, additional practical loadings, such as muscle force and dynamic activities, would be studied in future works. However, the applied loadings are quite fundamental, which could be the components of complicated loadings. Therefore, stress deterioration under all fundamental loadings is quite possible to appear under the complicated activities. The present study focused on the influence of tunnels on stress aggravation, and tried to eliminate the side effect of the graft and screws, thus, the material properties of the graft were assumed to be the same as that of the ACL. However, in reality, the graft may not be as strong as the natural ACL. This factor combined with tunnel creation may enlarge the tunnels further. The fixation was performed between the graft and tunnel wall, and the effect of the screws was neglected in the present study. The effect of the screw is mainly located at the extra-articular part of the tunnel; thus, only stress near the intra-articular tunnel aperture was considered in the present study. The wind wiper effect (sagittal tunnel-graft motion) was not considered due to the complications of FE convergence. However, in reality, the wind wiper effect could complicate the interaction between the graft and tunnel aperture, which would be investigated further.

In conclusion, both single-bundle and double-bundle ACL reconstructions cause stress deterioration in the subchondral bone. Stress in the lateral and posteromedial regions of the tibial single/AM tunnel was decreased, which could cause the collapse of the tunnel wall and contribute to tunnel enlargement; whereas, stress in the anterior region of tibial single/AM tunnel was increased, which may lead to the onset of OA. In particular, severe stress concentration occurred between the AM and PL tunnels in double-bundle case, which may contribute to tunnel communication. Moreover, the present study also finds that the concentration of tensile stress is transmitted from the articular surface to the middle of the tunnels; the tensile stress in the subchondral bone is decreased after reconstruction. The present study characterizes the stress deterioration around the intra-articular tunnel apertures after the single-bundle and double-bundle ACL reconstructions under different loading conditions. This study cannot arbitrarily conclude whether double-bundle is always better than single-tunnel reconstruction, but it indicates how tunnels disturb the stress environments, which can be quite severe after ACL reconstructions. These findings may provide knowledge to the pathomechanism of the bone tunnel enlargement and shall help improve surgical technique in the future.

CONCLUSION

Under the compression, von Mises stress was increased at anterior region of the single/AM tunnel,

while it was decreased at the lateral and posteromedial region of the single/AM tunnel in the tibial subchondral bone, which may contribute to the collapse of the tunnel wall and lead to bone tunnel enlargement. Tensile stress in the tibial subchondral plate was decreased after the ACL reconstruction. Double-bundle reconstruction further amplified the severity of stress concentration between the AM and PL tunnels, which may contribute to tunnel communication after surgery. The present study revealed that tunnel creations could significantly deteriorate the stress environment in the articular surface after single-bundle or double-bundle ACL reconstruction.

ACKNOWLEDGMENT

We thank Dr. Gong He for her very kind suggestions of the study design and results analysis, Dr. Kuang Guanming for advice on the surgery process, Dr. Wang Ting for advice on model development, and MR Henry Fong for editing manuscript. The present study was supported by grants from the National Natural Science Foundation of China (NSFC Grants 10925208 and 11120101001) and the National Key Lab of Virtual Reality Technology. The sponsors had no role in any aspect of the study, including data collection and analysis, manuscript preparation, or the authorization for publication.

CONFLICT OF INTEREST

We declare that the authors are not in any financial or personal relationship with people or organizations that may influence the present work; there is no professional or personal interest of any kind in any product, service, and/or company that may construe to influence the position presented in or the review of, the present manuscript.

REFERENCES

[1]Abaqus Analysis User's Manual. In: The Documentation for Abaqus 6.10, Vol. V, Part IX. USA: Simulia, Inc., pp. 34.1.2–3.

[2]Abaqus Analysis User's Manual. In: The Documentation for Abaqus 6.10, Vol. IV, Part VI. USA: Simulia, Inc., pp. 28.1.5–64.

[3]Au, A. G., *et al*. A three-dimensional finite element stress analysis for tunnel placement and buttons in anterior cruciate ligament reconstructions. *J. Biomech*. 38(4):827–832, 2005.

[4]Blankevoort, L., *et al*. Articular contact in a three-dimensional model of the knee. *J. Biomech*. 24(11):1019–1031, 1991.

[5]Boyd, S. K., R. Muller, and R. F. Zernicke. Mechanical and architectural bone adaptation in early stage experimental osteoarthritis. *J. Bone Miner. Res*. 17(4):687–694, 2002.

[6]Boyle, C., and I. Y. Kim. Three-dimensional micro-level computational study of Wolff's law via trabecular bone remodeling in the human proximal femur using design space topology optimization. *J. Biomech*. 44(5):935–942, 2011.

[7]Carter, D. R., T. Orr, and D. P. Fyhrie. Relationships between loading history and femoral cancellous bone architecture. *J. Biomech*. 22(3):231–244, 1989.

[8]Castañeda, S., J. Roman-Blas, R. Largo, and G. Herrero-Beaumont. Subchondral bone as a key target for osteoarthritis treatment. *Biochem. Pharmacol*. 83(3):315–323, 2011.

[9]Chhabra, A., *et al*. Anatomic, radiographic, biomechanical, and kinematic evaluation of the anterior cruciate ligament and its two functional bundles. *J. Bone Joint Surg. Am*. 88(Suppl 4):2–10, 2006.

[10]Donahue, T. L., *et al*. A finite element model of the human knee joint for the study of tibio-femoral contact. *J. Biomech. Eng*. 124(3):273–280, 2002.

[11]Ferretti, M., *et al*. Osseous landmarks of the femoral attachment of the anterior cruciate ligament: an anatomic study. *Arthroscopy* 23(11):1218–1225, 2007.

[12]Frost, H. M. A 2003 update of bone physiology and Wolff's Law for clinicians. *Angle Orthod*. 74(1):3–15, 2004.

[13]Fu, F. H., *et al*. Current trends in anterior cruciate ligament reconstruction. Part II. Operative procedures and clinical correlations. *Am. J. Sports Med*. 28(1):124–130, 2000.

[14]Fukubayashi, T., and H. Kurosawa. The contact area and pressure distribution pattern of the knee. A study of normal and osteoarthrotic knee joints. *Acta Orthop. Scand*. 51(6):871–879, 1980.

[15]Goulet, R. W., S. A. Goldstein, M. J. Ciarelli, J. L. Kuhn, M. B. Brown, and L. A. Feldkamp. The relationship between the structural and orthogonal compressive properties of trabecular bone. *J. Biomech*. 27(4):375–389, 1994.

[16]Huiskes, R., *et al*. Adaptive bone-remodeling theory applied to prosthetic-design analysis. *J. Biomech*. 20(11–12):1135–1150, 1987.

[17]Jagodzinski, M., *et al*. Analysis of forces of ACL reconstructions at the tunnel entrance: is tunnel enlargement a biomechanical problem? *J. Biomech*. 38(1):23–31, 2005.

[18]Kannus, P., and M. Jarvinen. Conservatively treated tears of the anterior cruciate ligament. Long-term results. *J. Bone Joint Surg. Am*. 69(7):1007–1012, 1987.

[19]Kopf, S., *et al*. Effect of tibial drill angles on bone tunnel aperture during anterior cruciate ligament reconstruction. *J. Bone Joint Surg. Am*. 92(4):871–881, 2010.

[20]Kopf, S., *et al*. The ability of 3 different approaches to restore the anatomic anteromedial bundle femoral insertion site during anatomic anterior cruciate ligament reconstruction. *Arthroscopy* 27(2):200–206, 2011.

[21]Kutzner, I., *et al*. Loading of the knee joint during activities of daily living measured in vivo in five subjects. *J. Biomech*. 43(11):2164–2173, 2010.

[22]Li, G., J. Suggs, and T. Gill. The effect of anterior cruciate ligament injury on knee joint function under a simulated muscle load: a three-dimensional computational simulation. *Ann. Biomed. Eng*. 30(5):713–720, 2002.

[23]Li, G., *et al*. A validated three-dimensional computational model of a human knee joint. *J. Biomech. Eng*. 121(6):657–662, 1999.

[24]Li, R. T., *et al*. Predictors of radiographic knee osteoarthritis after anterior cruciate ligament reconstruction. *Am. J. Sports Med*. 39(12):2595–2603, 2011.
[25]Louboutin, H., *et al*. Osteoarthritis in patients with anterior cruciate ligament rupture: a review of risk factors. *Knee* 16(4):239–244, 2009.
[26]Mellal, A., *et al*. Stimulating effect of implant loading on surrounding bone. Comparison of three numerical models and validation by in vivo data. *Clin. Oral Implants Res*. 15(2):239–248, 2004.
[27]Milz, S., and R. Putz. Quantitative morphology of the subchondral plate of the tibial plateau. *J. Anat*. 185:103–110, 1994.
[28]Netravali, N. A., *et al*. The effect of kinematic and kinetic changes on meniscal strains during gait. *J. Biomech. Eng*. 133(1):011006, 2011.
[29]Park, S., and G. A. Ateshian. Dynamic response of immature bovine articular cartilage in tension and compression, and nonlinear viscoelastic modeling of the tensile response. *J. Biomech. Eng*. 128(4):623–630, 2006.
[30]Pena, E., *et al*. A three-dimensional finite element analysis of the combined behavior of ligaments and menisci in the healthy human knee joint. *J. Biomech*. 39(9):1686–1701, 2006.
[31]Pombo, M. W., W. Shen, and F. H. Fu. Anatomic double-bundle anterior cruciate ligament reconstruction: where are we today? *Arthroscopy* 24(10):1168–1177, 2008.
[32]Radin, E. L., and R. M. Rose. Role of subchondral bone in the initiation and progression of cartilage damage. *Clin. Orthop. Relat. Res*. 213:34–40, 1986.
[33]Radin, E. L., *et al*. The role of bone changes in the degeneration of articular cartilage in osteoarthrosis. *Acta Orthop. Belg*. 44(1):55–63, 1978.
[34]Reilly, D. T., and A. H. Burstein. The elastic and ultimate properties of compact bone tissue. *J. Biomech*. 8(6):393–405, 1975.
[35]Sandberg, R., *et al*. Operative versus non-operative treatment of recent injuries to the ligaments of the knee. A prospective randomized study. *J. Bone Joint Surg. Am*. 69(8):1120–1126, 1987.
[36]Siebold, R. Observations on bone tunnel enlargement after double-bundle anterior cruciate ligament reconstruction. *Arthroscopy* 23(3):291–298, 2007.
[37]Song, Y., *et al*. A three-dimensional finite element model of the human anterior cruciate ligament: a computational analysis with experimental validation. *J. Biomech*. 37(3): 383–390, 2004.
[38]Taylor, M., K. E. Tanner, and M. A. Freeman. Finite element analysis of the implanted proximal tibia: a relationship between the initial cancellous bone stresses and implant migration. *J. Biomech*. 31(4):303–310, 1998.
[39]van Eck, C. F., *et al*. Anatomic single- and double-bundle anterior cruciate ligament reconstruction flowchart. *Arthroscopy* 26(2):258–268, 2010.
[40]Wilson, T. C., *et al*. Tunnel enlargement after anterior cruciate ligament surgery. *Am. J. Sports Med*. 32(2):543–549, 2004.
[41]Wolf, J. H. Julis Wolff and his ''law of bone remodeling''. *Orthopade* 24(5):378–386, 1995.
[42]Xu, Y., *et al*. Relation of tunnel enlargement and tunnel placement after single-bundle anterior cruciate ligament reconstruction. *Arthroscopy* 27(7):923–932, 2011.
[43]Yagi, M., *et al*. Biomechanical analysis of an anatomic anterior cruciate ligament reconstruction. *Am. J. Sports Med*. 30(5):660–666, 2002.
[44]Yao, J., *et al*. Stresses and strains in the medial meniscus of an ACL deficient knee under anterior loading: a finite element analysis with image-based experimental validation. *J. Biomech. Eng*. 128(1):135–141, 2006.